Available online at www.sciencedirect.com
SCIENCE DIRECT
Physica D 216 (2006) 95–102
PHYSICA D
www.elsevier.com/locate/physd

Bifurcation analysis of the localized modes dynamics in lattices with saturable nonlinearity

A. Maluckov[a,*], Lj. Hadžievski[b], M. Stepić[c]

[a] *Faculty of Sciences and Mathematics, Department of Physics, P.O.B. 224, 18001 Niš, Serbia and Montenegro*
[b] *Vinča Institute of Nuclear Sciences, P.O.B. 522, 11001 Belgrade, Serbia and Montenegro*
[c] *Institute of Physics and Physical Technologies, Clausthal University of Technology, D-38678 Clausthal-Zellerfeld, Germany*

Available online 6 March 2006

Abstract

The dynamics of localized modes in discrete media with saturable nonlinearity are investigated. The stability of stationary bright solitons is discussed from the view point of the energy minimum principle and mapping analysis. Due to the cascade saturation mechanism, a bifurcation from trapped to transversely moving localized mode is found for particular values of high power. The bifurcation coincides with the existence of the (almost) perfect separatrix in the corresponding area-preserving map. In addition, the definition of the Peierls–Nabarro effective potential is reconsidered.

Keywords: Cascade saturation; Bifurcation trapped-moving localized mode; Peierls–Nabarro potential

1. Introduction

In most cases of interest, the physical system corresponds to coupled sets of linear or nonlinear oscillators distributed in space, i.e. to the nonlinear lattice [1–3]. However, when a system length scale is much higher than the distance between the oscillators, continuous approximation is applicable. The physical system can then be mathematically modelled by nonlinear partial differential equations. If the system is integrable (possesses an infinite number of invariants) localized solutions of soliton type are possible. Moreover, the soliton-like solutions can also be found in nonintegrable continuous systems with a finite number of invariants. For example, localized solutions such as solitary waves, breathers, etc are detected experimentally and numerically in hydrodynamics, condensed matter physics, and biophysics [4].

In the opposite limit, characterized by a length scale comparable to the distance between the oscillators, the physical system should be modelled by a set of difference-differential equations. The interplay between nonlinearity and discreteness conspire to produce localized modes as discrete solitons, discrete breathers [5], etc. These modes arise naturally in the context of energy localization in discrete condensed matter and biological systems as well as in optical devices [3,6–8].

Generally, in discrete systems both continuous translation symmetry and integrability are broken. As a consequence, the localized solution is pinned in the lattice and free transverse steering of the localized modes cannot be sustained. The so-called pinned energy is related to the Peierls–Nabarro (PN) barrier [9–11]. Although the physical sense of the PN barrier is clear, there is no unique interpretation of its value [9,12]. This point will also be commented on in the present paper.

The stability of the localized modes in nonlinear lattices is considered from two aspects: the energy minimum principle and mapping orbit stability [13,14]. It is shown that physical systems described by the integrable discrete equation, such as the Ablowitz–Ladik (AL) equation, possess discrete soliton solutions that are manifested in the integrable map as perfect separatrices with coinciding stable and unstable manifolds [10, 15–17]. On the other hand, in the nonintegrable system (modelled by equations of the discrete nonlinear Schrödinger, DNLS, type) a separatrix is not perfect, in the sense that the stable and unstable manifolds no longer coincide but rather

* Corresponding author. Tel.: +381 18533015/loc.44; fax: +381 18 533 014.
E-mail address: maluckov@junis.ni.ac.yu (A. Maluckov).

0167-2789/$ - see front matter © 2006 Elsevier B.V. All rights reserved.
doi:10.1016/j.physd.2005.12.011

intersect each other transversely in homoclinic points, creating complex chaotic dynamics that eventually develop Smale horseshoes. The change between the perfect and imperfect map separatrix with a change of the parameter values is interpreted as an increasing value of the PN barrier from the zero level [15]. This is closely related to the possibility for transverse steering of the localized modes in discrete nonlinear lattices. Free steering is allowed in integrable systems [13,18,19] and in nonintegrable systems with weakly destroyed translational symmetry. But the mobility of the strongly localized modes is still an open question.

Here, the dynamics of localized modes in discrete media with saturable nonlinearity, such as waveguide arrays in photorefractive strontium barium niobate crystals, are investigated. The physics of localized modes in photorefractive media is based on the electro-optic effect. Self-trapping usually requires a DC electric field [20]. Briefly, the illumination of the photorefractive crystal initiates charge generation, and thus the formation of an internal space electric field. The electric field changes the refractive index via the electro-optic effect and generates charge drift in the opposite direction with respect to the charge diffusion, until equilibrium is established. The charge drift also can be forced by an external electric field. The net effect leads to the saturable nature of the underlying nonlinearities.

In previous publications, investigations of localized modes in photorefractive media started with the study of the existence and stability of discrete solitons [21,22]. The saturable nonlinearity strongly affects soliton stability properties and its propagation across the lattice. It is revealed that the behaviour of localized modes in photorefractive media differs considerably from those of discrete lattices with cubic (Kerr) nonlinearity [12,23]. A deeper understanding of these differences is now a crucial topic. The present paper is organized in the following manner. A brief description of the model and previously obtained results concerning the existence of the localized modes in photorefractive media with saturable nonlinearity are given in Section 2. In addition, in Section 2.1 the applied numerical methods and the definition of the Liapunov exponent are presented. In Section 3, the stability of the localized modes with respect to longitudinal and transversal perturbations is considered, adopting the dynamical and mapping stability analysis. The most significant phenomenon is bifurcation from the trapped to the moving state, which is discussed in detail in Section 4. The conclusions are summarized in the last part.

2. Establishment of the model

The one-dimensional DNLS lattice model with saturable nonlinearity, which represents a discrete version of the Vinetskii–Kukhtarev equation [24], is investigated:

$$\mathrm{i}\frac{\partial U_n}{\partial t} + (U_{n+1} + U_{n-1} - 2U_n) - \gamma\frac{U_n}{1+|U_n|^2} = 0. \tag{1}$$

Here, U_n is the wave function in the n-th lattice element ($n = 1, \ldots, N$) with ($U_{N+1} = U_1$) for the case of periodic boundary conditions, and γ is the nonlinearity parameter [22].

The above equation represents a system of linearly coupled nonlinear difference-differential equations that are not integrable but possess two conserved quantities: Hamiltonian $H = \sum_n[\gamma \ln(1 + |U_n|^2) + |U_{n-1} - U_n|^2]$ and power $P = \sum_n |U_n|^2$.

Discrete stationary localized modes of the bright soliton type can be obtained from Eq. (1), assuming the solution in a form $U_n(z) = \phi_n \mathrm{e}^{-\mathrm{i}\omega t}$ and obtaining a set of coupled algebraic equations for the real function ϕ_n [22]

$$\omega\phi_n + (\phi_{n+1} + \phi_{n-1} - 2\phi_n) - \frac{\gamma\phi_n}{1+|\phi_n|^2} = 0, \tag{2}$$

where ω is the propagation parameter. From Eq. (2), different types of localized modes can be obtained. Here, two types of localized bright solitons are investigated: on-site solitons centered at the lattice site $n = 0$,[1] and inter-site solitons centered between two neighboring lattice elements $n = \pm 1$ (modes A and B in paper [22], respectively). The existence of the localized modes is investigated in paper [22]. It is shown that the bright solitons exist in the parameter region $\omega \leq \gamma$.

2.1. Numerical model

Optical pulse propagation in the nonlinear lattice (1) is solved numerically using the 6th order Runge–Kutta procedure. The following parameter set is chosen[2]: $\gamma = 2$, 3.05, 6.1, 9.1, 12.1 and 25.

The mapping stability analysis in Section 3.2, i.e. the stability of the fixed points of the corresponding 2D map, is performed by an iterative procedure. Map dynamics is followed in the corresponding phase space for $M = 1000$ mapping trajectories randomly initialized in the neighborhood of the fixed point.

In addition, the effective Liapunov exponent (LE) as a measure of the increasing map stochasticity is calculated using the procedure developed in the literature [25]. The Liapunov exponent of the jth trajectory is defined as [25]:

$$l_j(t) \equiv \frac{1}{t}\ln\left(\frac{d_j(t)}{d_j(t=0)}\right), \tag{3}$$

where $d_j(t)$ is the distance at time $t = jdt$ between two initially neighboring trajectories, usually evaluated in the tangential space of the trajectory [26]. The positive value of the LE, $l_j > 0$, denotes exponential separation of two initially neighboring trajectories. On the other hand, $l_j \leq 0$ corresponds to initially neighboring trajectories stuck to each other. The effective LE is defined as the averaged LE over different initial conditions (index j):

$$L(t) \equiv \langle l_j(t)\rangle = \frac{1}{M}\sum_{j=1}^{M} l_j(t). \tag{4}$$

[1] The numeration $n = \ldots, -2, -1, 0, 1, 2, \ldots$ for on-site and $n = \ldots, -2, -1, 1, 2, \ldots$ for inter-site localized modes is taken from Ref. [22].

[2] This set belongs to the corresponding experimental range of physical parameters: the electric field, $E = (0\text{–}10)$ kV/cm, the wavelength of the laser light, $\lambda = (480\text{–}520)$ nm, and the distance between two adjacent lattice elements of the order of several μm.

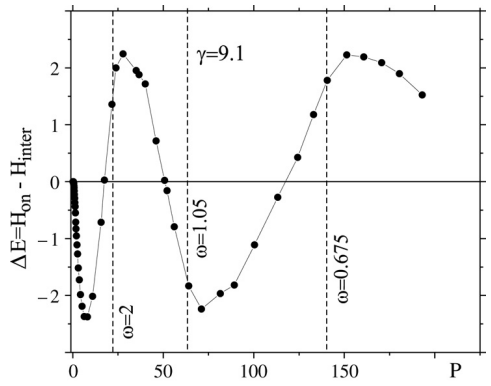

Fig. 1. The energy difference, ΔE, i.e. the value of the Peierls–Nabarro effective potential barrier, ΔE_{PN} (Section 3.1), vs the total power P for $\gamma = 9.1$. The straight lines on the graph denote the powers that correspond to the potentially moving localized modes.

3. Stability of localized modes

First of all, the (dynamical) stability of the physical solutions and the stability of the corresponding map orbit (linear mapping) have to be distinguished [9,10,18]. A dynamically stable solution minimizing the action (energy) corresponds to a linearly unstable map orbit, whereas physically unstable solutions corresponding to the maximum energy configuration are reflected in the map dynamics as linearly stable map orbits.

3.1. Dynamical stability analysis

In the case of coexisting stationary modes with fixed power, according to the energy minimum criterion, the stable mode is the mode with the minimum energy.[3] Here, observing the energy difference between the two coexisting modes with the same power, the on-site and inter-site bright solitons,

$$\Delta E = H_{\mathrm{on}}(P) - H_{\mathrm{inter}}(P), \tag{5}$$

the stable on-site (inter-site) mode corresponds to the negative (positive) value of ΔE (Fig. 1). The shape of the ΔE vs P curve, which is characterized by several zeros, is determined by the effect of the saturable nonlinearity [22]. Accordingly, in the range of small γ, where saturable nonlinearity cannot significantly affect the system behaviour, vanishing values of the ΔE for all P are observed. The stability of the localized mode is checked numerically by adding small in-phase perturbation to the unperturbed stationary bright soliton. Unstable on-site and inter-site localized modes propagate as stable inter-site and on-site localized breathers with the same power, respectively [22]. The regions with $\Delta E \approx 0$ are characterized by the marginal stability of both mentioned modes.

From the view point of the localized mode transverse mobility, the energy difference is associated with the Peierls–Nabarro effective potential, which originates from the dynamical studies of the kink solutions [9,12], $\Delta E = \Delta E_{PN}$. The amplitude of the PN potential is considered to be equal to the minimum barrier that must be overcome to translate the center of mass of the system by half a lattice period. Note that, in this context, the on-site and inter-site localized modes of the same power are treated as two dynamical realizations of the one moving mode. However, the above definition deserves caution in the case of a moving breather, which inherently has the internal structure, as is shown in the following.

The transverse propagation of the localized modes is numerically initiated by adding the small transverse perturbation as a phase shift of the form $\exp(\mathrm{i}kn)$, where parameter k is the initial transverse mode velocity. Perturbation can initiate translational movement of dynamically unstable (according to the minimum energy criterion) on-site or inter-site modes of the fixed power.

The shape of the observed PN potential (bounded potential with multiple zeros Fig. 1) is related to the cascade amplitude saturation; Figs. 2 and 3 [22]. Precisely, increasing P does not lead to continuous energy localization into the single lattice element and decoupling from the rest of the lattice, as in the case of the DNLS with cubic nonlinearity. The cascade saturation suppresses the energy localization resulting in the existence of less localized modes as P increases (Fig. 2).

Finally, the shape of the PN potential influences the power dependent steering of the localized mode across the lattice. The fact that the amplitude of the PN potential barrier is bounded has brought the general conclusion that the ability of the large power solitons to move across the lattice is considerably higher than in the case of DNLS lattices with cubic nonlinearity. The significant point is that the on-site and inter-site stationary solitons, without internal oscillations but with different self-frequencies for the fixed power P, propagate transversely as the corresponding breathers characterized by the self-frequency between ω_{on} and ω_{inter}.[4]

The most intriguing open question is the interpretation of free steering of localized modes with high power (the effect is absent in the DNLS lattice with cubic nonlinearity); Fig. 4(d). In addition, rigidity of the localized modes around the zeros of the PN potential in the high power region, Fig. 1, influences the reconsideration of the PN potential given by Eq. (3).

An interesting view on the transition (bifurcation) trapped-moving localized mode can be obtained in the space $(\omega, \gamma, P(H))$; Fig. 5. The $P(\omega)$ and $H(\omega)$ curves for both on-site and inter-site modes are monotonically decreasing with ω and are concave except in the 'turning' points $\omega = 0.675, 2$ for the on-site mode and 1.05 for the inter-site mode, which are correlated with the nature of the saturable nonlinearity; Fig. 6. Only the localized modes with high power for these parameter values can bifurcate to the corresponding moving localized breathers; Fig. 4(d), (e). Note that the particular regions are not analytically reachable (the regions of high power [22]). The dynamics in the turning point is associated with the cascade

[3] Note that the stability criterion is the energy maximum principle in the self-defocusing media [16] instead of the energy minimum principle in the self-focusing media.

[4] Note that, except for the breather with a single self-frequency, the quasi-periodic and chaotic breathers can be realized.

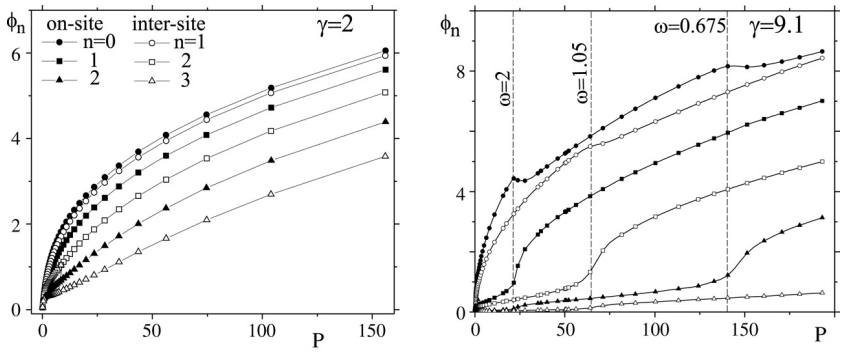

Fig. 2. Amplitude versus total power. Increasing the parameter γ ($\omega \leq \gamma$ for fixed γ), the cascade saturation mechanism significantly affects the dynamics of localized modes. In the case with $\gamma = 2$, transversely kicked localized modes of all powers freely move across the lattice. On the other hand, for $\gamma = 9.1$, mobility is observed only for modes with $\gamma \approx \omega$ ($P \ll 1$) and $\omega = 0.675, 1.05, 2$ ($P \gg 1$), which are indicated by the dashed lines on the graph.

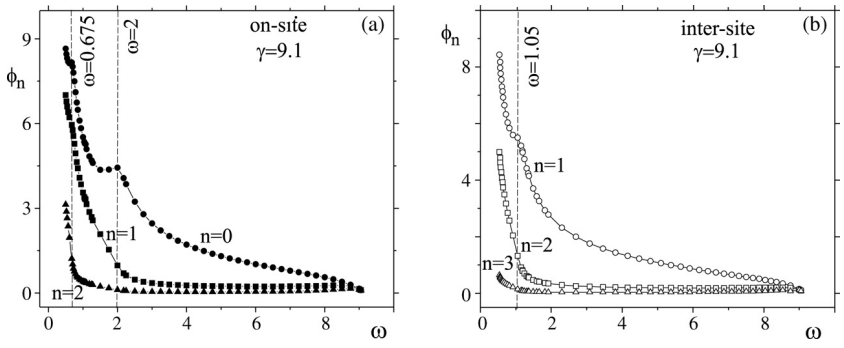

Fig. 3. Amplitude versus the propagation parameter for on-site and inter-site localized modes. The dashed lines indicate the critical values of the parameter ω: 0.675, 2 for the on-site mode (a) and 1.05 for the inter-site mode (b). Only the modes for critical ω can be moved across the lattice.

nature of amplitude saturation, as the comparison of Fig. 6 with Fig. 2 (the curves amplitude vs P) illustrates.

3.2. Mapping stability

It is convenient to cast the real-valued second order difference Eq. (2) into a two-dimensional map $R^2 \to R^2$ by defining $x_n = \phi_n$ and $y_n = \phi_{n-1}$, where the lattice index plays the role of discrete 'time'. The corresponding map M can be given as:

$$\begin{aligned} x_{n+1} &= \left(2 - \omega + \frac{\gamma}{1 + x_n^2}\right) x_n - y_n \\ y_{n+1} &= x_n. \end{aligned} \tag{6}$$

Reversibility of the map M is established by factorization $\mathsf{M} = \mathsf{M}_0\mathsf{M}_1$ with M_0

$$\begin{aligned} \overline{x} &= y \\ \overline{y} &= x, \end{aligned} \tag{7}$$

and with M_1

$$\begin{aligned} \overline{x} &= x \\ \overline{y} &= \left(2 - \omega + \frac{\gamma}{1 + x_n^2}\right) x - y, \end{aligned} \tag{8}$$

where $\mathsf{M}_0, \mathsf{M}_1$ are involutions and their corresponding symmetry lines are given by $S_0: x = y$ and $S_1: -[2 - \omega + \gamma/(1+x^2)]x/2$. The map M is an analytic area-preserving twist map [13].

To investigate the stability of stationary localized solutions in the form of bright solitons, the study of the fixed points (period-1 orbits) of the map M, Eq. (6), is sufficient. The fixed points, for which $x = y$, are located at:

$$x_0 = 0, \qquad x_{1,2} = \pm\sqrt{\frac{\gamma - \omega}{\omega}}. \tag{9}$$

The last two fixed points exist only if $\mathrm{sgn}(\gamma - \omega) = \mathrm{sgn}(\omega)$, i.e. if $\gamma \geq \omega, \omega > 0$ or $\gamma \leq \omega, \omega < 0$. Here, the first case is simulated. The stability of the fixed points is governed by their values for the corresponding residues [13]:

$$\rho = \frac{1}{4}\left(2 - \mathrm{Tr}(\mathsf{DM})\right), \tag{10}$$

where the tangent map DM is determined by:

$$\mathsf{DM} = \begin{bmatrix} \omega_n & -1 \\ 1 & 0 \end{bmatrix} \tag{11}$$

with

$$\omega_n = 2 - \omega + \gamma \frac{1 - x_n^2}{(1 + x_n^2)^2}. \tag{12}$$

The value of residue at fixed point $x_0 = 0$ is

$$\rho = \frac{1}{4}(\omega - \gamma), \tag{13}$$

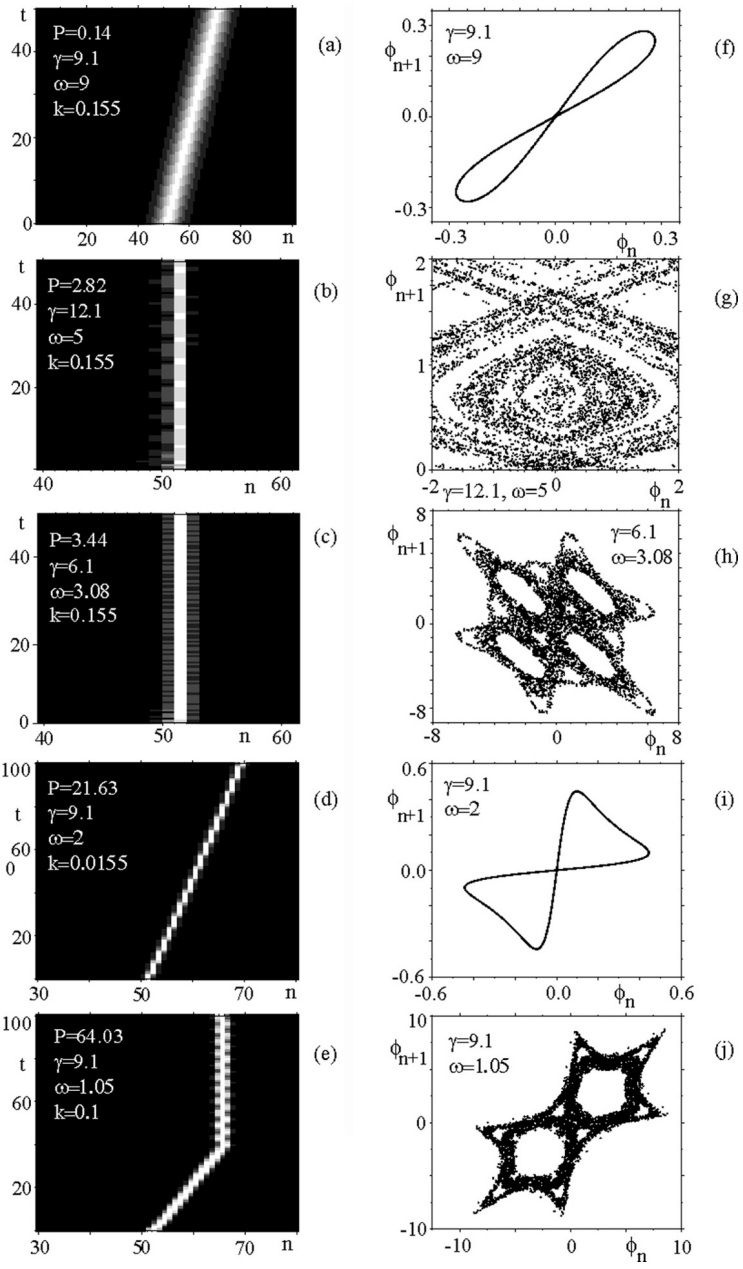

Fig. 4. The bifurcation trapped-moving localized mode (breather). The 2D plots of the transversely kicked localized mode and the corresponding map orbits around the fixed point (0, 0) are shown on the left and right, respectively. The moving localized mode exists for $\omega \approx \gamma$ (a,f) and $\omega = 2$ independently on γ (d,i). Transient mobility is observed for $\omega = 1.05$ and $k = 0.1$ (e,j). Initially, the on-site mode is centered at $n = 51$ and the inter-site mode between $n = 51$ and $n = 52$.

and at fixed points $x_{1,2}$ it is

$$\rho = \frac{\omega}{2\gamma}(\gamma - \omega). \tag{14}$$

For the actual sets of parameters where $0 < \omega \leq \gamma$, at x_0 the residue passes through zero, i.e. $\rho \leq 0$, and hence the origin losses stability. The calculation of normal forms shows that at $\omega \approx \gamma$ the origin is turned into an unstable hyperbolic point caused by a tangent (saddle-node) bifurcation; Fig. 7(a). The hyperbolic point is connected to itself by a homoclinic orbit created by the (invariant) unstable and stable manifold. The nonlinear stability analysis proved that the homoclinic orbit is manifested on the lattice chain as a soliton-like solution [9]. There exist two homoclinic orbits: the homoclinic orbit crossing S_0, which corresponds to the inter-site mode (Fig. 4(f)), and the homoclinic orbit with three large amplitudes, which corresponds to the on-site mode (Fig. 4(j)).

The pair of fixed points $x_{1,2}$ on the symmetry line S_0 form stable elliptic fixed points according to the value of the residue $0 < \rho < 1$ for the actual parameter region; Fig. 7(b).

Generally, stable stationary localized solutions are related to homoclinic and heteroclinic orbits of the corresponding map, even though there exist neighboring map orbits that are strongly chaotic. The reason is that the localized states rely on the structural stability of orbits homoclinic or heteroclinic to unstable hyperbolic fixed points. With the exception of the

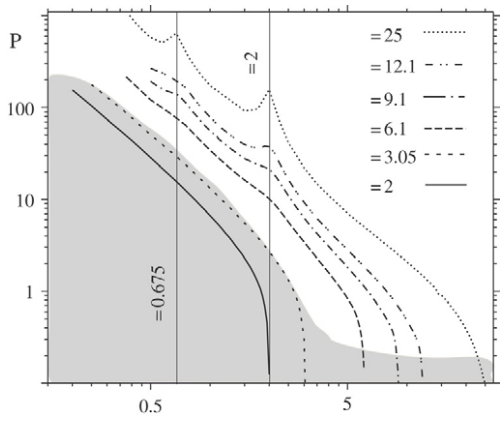

Fig. 5. The total power of on-site localized modes as a function of parameter ω for different γ in log–log proportions. The moving localized modes are observed for the critical values of parameter ω, i.e. at turning points (straight lines), and in the shadowed region of the plot.

P values around turning points, the increasing stochasticity with increasing P, i.e. with a decreasing value of ω from the bifurcating value, $\omega \approx \gamma$, is clearly seen by plotting the map orbits initialized near the corresponding fixed point; Figs. 4(g), (h). This is quantified by calculating the effective LE [27] (Section 2.1). A two dimensional area-preserving map is characterized by two one-dimensional LE, $L_1 = -L_2$, or by a zeroth two-dimensional LE [25]. Here, the non-negative 1D LE is followed. The effective LE as a function of the total power P is plotted in Fig. 8. As can be seen, homoclinic orbits that correspond to perfect separatrices are characterized with $L \to 0$. In the presence of imperfect separatrices, L slowly decreases, saturating to small finite positive value. Finally, highly stochastic map orbits are characterized by the fast saturation of the L to the significant finite positive value.

The existence of the moving localized modes coincides with the appearance of the nearly perfect mapping separatrices, as noted above. In all other parameter regions, the localized mode (breather) is trapped between two adjacent lattice elements.

4. Bifurcation trapped-moving localized mode: Discussion

The existence of moving soliton-like modes and breathers as mathematically exact solutions is still an open question [15, 19]. Here, an attempt is made to qualify the genesis of the moving modes in discrete photorefractive media with saturable nonlinearity.

In order to better understand the unusual dynamical behaviour of localized mode, which is reported in reference [22], the stationary Eq. (2) is multiplied by the term $1+\phi_n^2$ and rewritten as:

$$(\omega - 2 - \gamma)\phi_n + (\phi_{n+1} + \phi_{n-1})(1 + \phi_n^2) + (\omega - 2)\phi_n^3 = 0. \tag{15}$$

This coincides with the stationary generalized discrete nonlinear Schrödinger (GDNLS) equation in reference [13] ($V = 1$, $\mu = 1$).

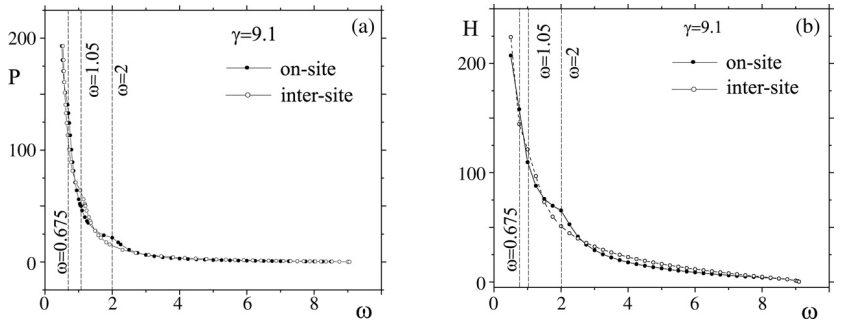

Fig. 6. The total power and Hamiltonian as functions of the parameter ω for $\gamma = 9.1$. The dashed lines denote the parameter values at which the transverse moving localized mode exists.

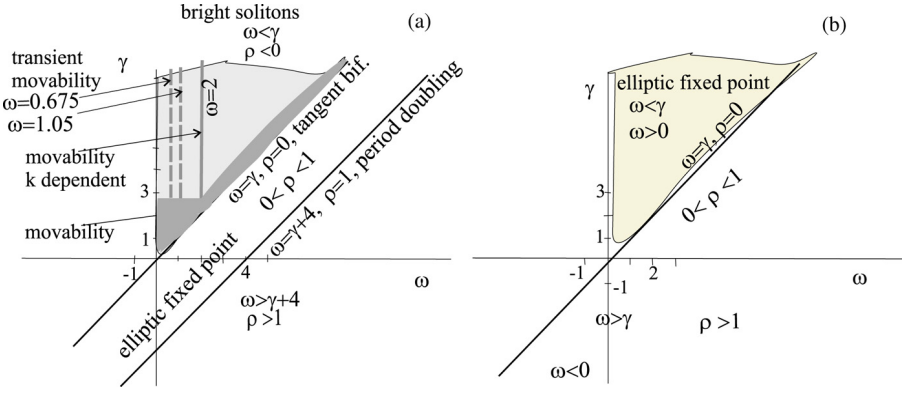

Fig. 7. The bifurcation diagram in parameter space (γ, ω). The existence region of the stationary bright solitons, $\omega \leq \gamma$, and the region where the moving localized mode can be excited are shadowed. Parts (a) and (b) illustrate the behaviour near the fixed points x_0 and $x_{1,2}$, respectively.

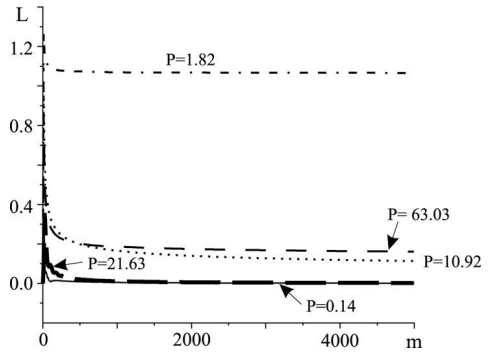

Fig. 8. Effective Liapunov exponent for $\gamma = 9.1$ and different P. Values $P = 0.14$, 1.82, 10.92, 21.63 and 63.03 correspond to $\omega = 9$, 5, 2.5, 2 and 1.05, respectively. Index m notes the number of steps in numerical simulation.

At the value of the propagation parameter, $\omega = 2$, the stationary version of the discrete, integrable AL equation [13] is obtained from Eq. (15). The corresponding map orbits around the origin are perfect separatrices. In the near neighborhood of $\omega = 2$, the last term in (15) can be considered as a small perturbation of the stationary AL equation. The perturbed map orbits around the origin are imperfect separatrices, i.e. the stable and unstable manifolds of the fixed point at the origin transversely intersect each other. The Melnikov analysis, as in Ref. [13], shows that the distance between two adjacent transverse intersections of the stable and unstable manifolds of the (0, 0) fixed point depends on the value of $\omega - 2 - \gamma$:

$$\Delta \approx \ln\left(-\frac{\omega-2-\gamma}{2}+\sqrt{\frac{(\omega-2-\gamma)^2}{4}-1}\right). \tag{16}$$

The perfect separatrix corresponds to $\omega(\approx 2) = \gamma$, i.e. to the bifurcation at the fixed point (0, 0) (Section 3.2). Numerical calculations in the parameter range $0 < \omega \leq \gamma < 3$ (Fig. 5) show that the localized modes of all powers can be moved across the lattice. Thus, the mobility can be related to the existence of the perfect or transversely intersecting separatrices of the corresponding mappings [9] when the stochasticity is not yet significantly developed. This is concluded from the vanishing of the Liapunov exponents.

Increasing the value of γ ($\omega \leq \gamma$, according to the existence condition), the mobility is sustained in two cases; Figs. 5 and 7. The first corresponds to the localized modes with low power, $P < 1$ and $\omega \approx \gamma$. This is the neighborhood of the first zero of the ΔE_{PN}; Fig. 1. The second is related to the localized modes with high power, $P \gg 1$, at turning points of the curve P vs ω; Figs. 5 and 6. There, the corresponding map orbits are nearly perfect separatrices (Section 3.2) and the $E_{PN} \neq 0$ (Fig. 1). Thus, the nonintegrability of the map and the resulting transverse intersection of the stable and unstable manifolds at an unstable fixed point means that the localized solutions cannot be translated over the lattice from one point to an adjacent point without overcoming an energy barrier. This energy barrier is associated with the PN potential barrier. Now, the minimum of the PN barrier (zeroth value) is in the parameter range where the map orbit is a perfect separatrix.

Let us summarize basic facts about map orbit's behaviour near the separatrices in the context of the moving localized modes.

- *Region of small power*

  In the region of small power, $P \ll 1$, model equations (1) are nicely approximated by the discrete nonlinear Schrödinger equations with cubic nonlinearity [12,23]. The solitons are characterized here by large width (tens of lattice elements). Roughly, the coarse grained continuity of the lattice system is established. Thus, in spite of the nonintegrability and broken translational symmetry (due to discreteness) the stationary discrete localized modes (soliton-like solutions) can be steered transversely through the lattice (Fig. 4(a)). The steering efficiency is a function of both P and k.

  From the view point of the mappings, the invariant map orbits are nearly perfect separatrices; Fig. 4(f). A small perturbation is a seed for overcoming the separatrix and for generating the transverse movement [22]. Steering efficiency can be controlled through the value of k (the steering velocity). In addition, the effective LE saturates to nearly the zeroth value; Fig. 8.
- *Intermediate and high powers: The critical points*

  The most significant property of the saturable nonlinearity in the present model is the cascade nature of saturation; Figs. 2 and 3. Generally, as written in Section 3, when the increase of the amplitude in the central element stops (i.e. the amplitude locally saturates) the power increase is maintained by the increase of the amplitude in the first several neighboring elements. At the corresponding parameter values, the power and energy curves possess turning points; Fig. 6. Locally, this parameter range is characterized by marginal mode stability and the new quality in the soliton dynamics is proclaimed.

  It is worth stressing once more that the critical (turning) points correspond to $\omega = 0.675$, 1.05 and 2 independently of γ. Above the threshold value of k, the trapping-moving exchange starts. However, free moving breathers are found for some value of k and $\omega = 2$, due to the recovered integrability of the system which is described by the AL type Eq. (15). Then, the perfect separatrix appears in the corresponding phase diagram[5]; Fig. 4(h).

  At the points $\omega = 0.675$, 1.05, the corresponding phase diagrams are characterized by the net of separatrices, i.e. interrelated stochasticity regions, as illustrated in Fig. 4(j). Stochasticity layers of finite width are associated with the transient mobility for some values of parameter k. A deeper understanding of the dynamics at these points is deserving of additional analysis.
- *Intermediate and high powers: Far from the critical points*

  The leading role in the power increase is played by the amplitude in the central lattice element (element index $n =$

[5] In Refs. [9,10], the presence of separatrices is associated with phenomenological recovery of the translational symmetry in the discrete system.

0, or $|n| = 1$ for on-site or inter-site stationary solitons, respectively (Section 2)). The power and energy curves are concave, and monotonically decreasing with the increasing parameter ω; Figs. 5 and 6.

For all P in this region independently of the values of ω, k, the localized mode (breather) is trapped on the lattice element. The corresponding map orbits around the unstable fixed point (at the origin) are highly stochastic, or develop complex stochastic nets for modes with high power far from or near to the critical points, i.e. the turning points, respectively (Fig. 4(g), (h)). This is indicated by the finite non-negative value of the effective LE; Fig. 8. From the view point of the modified PN potential, its value is now finite and modes are pinned by the lattice elements.

5. Conclusions

In the present paper, the dynamics of bright localized modes in discrete media with saturable nonlinearity are investigated numerically. The stability properties of these modes are considered from the view point of both the dynamical stability and the corresponding map orbit stability. The main result is an improved understanding of the bifurcation from trapped to moving localized modes of high power. This bifurcation is generically related to the cascade mechanism of saturation and, as such, does not exist in the discrete media with cubic nonlinearity.

It is shown that the bifurcation from trapped to moving localized modes of high power does not occur at the zeroes of the effective Peierls–Nabarro potential barrier, defined as the energy difference between the on-site and inter-site localized modes of the same power. Rather, the bifurcation appears for the specific values of parameters where the corresponding map orbit is an (almost) perfect separatrix. An intriguing future task will be to study the interactions of strongly localized modes within the approaches developed here.

Acknowledgements

This work is carried out under the auspices of the Ministry of Sciences and Protection of the Environment of the Republic of Serbia (project 1964). The authors thank M. Škorić and M. Rajković for valuable discussions.

References

[1] D.N. Christodoulides, R.I. Joseph, Opt. Lett. 13 (1988) 794.
[2] V. Ahufinger, A. Sanpera, P. Pedri, L. Santos, M. Lewenstein, Phys. Rev. A 69 (2004) 053604.
[3] E. Trias, J.J. Mazo, T.P. Orlando, Phys. Rev. Lett. 84 (2000) 741.
[4] E.A. Kuznetzov, A.M. Rubenchik, V.E. Zakharov, Phys. Rep. 142 (1986) 103.
[5] R.S. MacKay, S. Aubry, Nonlinearity 7 (1994) 1623.
[6] B.I. Swanson, J.A. Brozik, S.P. Love, G.F. Strouse, A.P. Shreve, A.R. Bishop, W.Z. Wang, M.I. Salkola, Phys. Rev. Lett. 82 (1999) 3288.
[7] M. Peyrard, Nonlinearity 17 (2004) R1.
[8] J. Coste, J. Peyraud, Phys. Rev. B 39 (1989) 13086.
[9] S. Aubry, Physica D 7 (1983) 240.
[10] D. Hennig, G.P. Tsironis, Phys. Rep. 307 (1999) 333.
[11] D.E. Pelinovsky, A.A. Sukhorukov, Yu.S. Kivshar, Phys. Rev. E 70 (2004) 036618.
[12] Yu.S. Kivshar, D.K. Campbell, Phys. Rev. E 48 (1993) 3077.
[13] D. Hennig, K.Ø. Rasmussen, H. Gabriel, A. Bülow, Phys. Rev. E 54 (1996) 5788.
[14] K. Furuya, A.M. Ozorio de Almeida, J. Phys. A: Math. Gen. 20 (1987) 6211.
[15] S. Aubry, Physica D 103 (1997) 201–250.
[16] R. Carretero-Gonzalez, K. Promislow, Phys. Rev. A 66 (2002) 033610.
[17] S. Wiggins, Global Bifurcations and Chaos: Analytical Methods', Springer-Verlag, New York, 1988.
[18] S. Flach, C.R. Willis, Phys. Rep. 295 (1998) 181.
[19] D. Chen, S. Aubry, G.P. Tsironis, Phys. Rev. Lett. 77 (1996) 4776.
[20] M. Segev, G.C. Valley, B. Crosignani, P. DiPorto, A. Yariv, Phys. Rev. Lett. 73 (1994) 3211.
[21] M. Stepić, D. Kip, Lj. Hadžievski, A. Maluckov, Phys. Rev. E 69 (2004) 066618.
[22] Lj. Hadžievski, A. Maluckov, M. Stepić, D. Kip, Phys. Rev. Lett. 93 (2004) 033901.
[23] K. Morandotti, U. Peschel, J.S. Aitchison, H.S. Eisenberg, Y. Silberberg, Phys. Rev. Lett. 83 (1999) 2726.
[24] V.O. Vinetskii, N.V. Kukhtarev, Sov. Phys. Solid State 16 (1975) 2414.
[25] A.J. Lichtenberg, M.A. Lieberman, Regular and Chaotic Dynamics, Springer-Verlag, New York, 1992.
[26] G. Benettin, L. Galgani, J-H. Strelcyn, Phys. Rev. A 14 (1976) 2338.
[27] A. Maluckov, N. Nakajima, M. Okamoto, S. Murakami, R. Kanno, Physica A 322 (2003) 13.